JOURNAL OF Applied Polymer SCIENCE

Special Issue: Microfiltration and Ultrafiltration Membrane Science and Technology

Guest Editors: Prof. Isabel C. Escobar (University of Toledo) and Prof. Bart Van der Bruggen (University of Leuven)

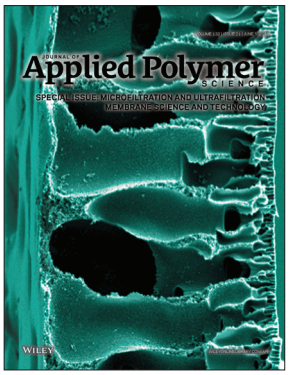

EDITORIAL

Microfiltration and Ultrafiltration Membrane Science and Technology
I. C. Escobar and B. Van der Bruggen, *J. Appl. Polym. Sci.* 2015, **DOI: 10.1002/app.42002**

REVIEWS

Nanoporous membranes generated from self-assembled block polymer precursors: *Quo Vadis*?
Y. Zhang, J. L. Sargent, B. W. Boudouris and W. A. Phillip, *J. Appl. Polym. Sci.* 2015, **DOI: 10.1002/app.41683**

Making polymeric membranes anti-fouling via "grafting from" polymerization of zwitterions
Q. Li, J. Imbrogno, G. Belfort and X.-L. Wang, *J. Appl. Polym. Sci.* 2015, **DOI: 10.1002/app.41781**

Fouling control on MF/ UF membranes: Effect of morphology, hydrophilicity and charge
R. Kumar and A. F. Ismail, *J. Appl. Polym. Sci.* 2015, **DOI: 10.1002/app.42042**

EMERGING MATERIALS AND FABRICATION

Preparation of a poly(phthalazine ether sulfone ketone) membrane with propanedioic acid as an additive and the prediction of its structure
P. Qin, A. Liu and C. Chen, *J. Appl. Polym. Sci.* 2015, **DOI: 10.1002/app.41621**

Preparation and characterization of MOF-PES ultrafiltration membranes
L. Zhai, G. Li, Y. Xu, M. Xiao, S. Wang and Y. Meng, *J. Appl. Polym. Sci.* 2015, **DOI: 10.1002/app.41663**

Tailoring of structures and permeation properties of asymmetric nanocomposite cellulose acetate/silver membranes
A. S. Figueiredo, M. G. Sánchez-Loredo, A. Maurício, M. F. C. Pereira, M. Minhalma and M. N. de Pinho, *J. Appl. Polym. Sci.* 2015, **DOI: 10.1002/app.41796**

LOW-FOULING POLYMERS

Low fouling polysulfone ultrafiltration membrane via click chemistry
Y. Xie, R. Tayouo and S. P. Nunes, *J. Appl. Polym. Sci.* 2015, **DOI: 10.1002/app.41549**

Elucidating membrane surface properties for preventing fouling of bioreactor membranes by surfactin
N. Behary, D. Lecouturier, A. Perwuelz and P. Dhulster, *J. Appl. Polym. Sci.* 2015, **DOI: 10.1002/app.41622**

PVC and PES-*g*-PEGMA blend membranes with improved ultrafiltration performance and fouling resistance
S. Jiang, J. Wang, J. Wu and Y. Chen, *J. Appl. Polym. Sci.* 2015, **DOI: 10.1002/app.41726**

Improved antifouling properties of TiO_2/PVDF nanocomposite membranes in UV coupled ultrafiltration
M. T. Moghadam, G. Lesage, T. Mohammadi, J.-P. Mericq, J. Mendret, M. Heran, C. Faur, S. Brosillon, M. Hemmati and F. Naeimpoor, *J. Appl. Polym. Sci.* 2015, **DOI: 10.1002/app.41731**

Development of functionalized doped carbon nanotube/polysulfone nanofiltration membranes for fouling control
P. Xie, Y. Li and J. Qiu, *J. Appl. Polym. Sci.* 2015, **DOI: 10.1002/app.41835**

JOURNAL OF Applied Polymer SCIENCE

Special Issue: Microfiltration and Ultrafiltration Membrane Science and Technology

Guest Editors: Prof. Isabel C. Escobar (University of Toledo) and
Prof. Bart Van der Bruggen (University of Leuven)

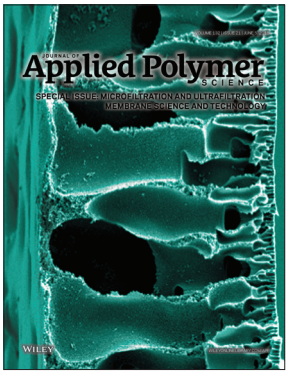

SURFACE MODIFICATION OF POLYMER MEMBRANES

Highly chlorine and oily fouling tolerant membrane surface modifications by *in situ* polymerization of dopamine and poly(ethylene glycol) diacrylate for water treatment
K. Yokwana, N. Gumbi, F. Adams, S. Mhlanga, E. Nxumalo and B. Mamba, *J. Appl. Polym. Sci.* 2015, **DOI: 10.1002/app.41661**

Fouling control through the hydrophilic surface modification of poly(vinylidene fluoride) membranes
H. Jang, D.-H. Song, I.-C. Kim, and Y.-N. Kwon, *J. Appl. Polym. Sci.* 2015, **DOI: 10.1002/app.41712**

Hydroxyl functionalized PVDF-TiO_2 ultrafiltration membrane and its antifouling properties
Y. H. Teow, A. A. Latif, J. K. Lim, H. P. Ngang, L. Y. Susan and B. S. Ooi, *J. Appl. Polym. Sci.* 2015, **DOI: 10.1002/app.41844**

Enhancing the antifouling properties of polysulfone ultrafiltration membranes by the grafting of poly(ethylene glycol) derivatives via surface amidation reactions
H. Yu, Y. Cao, G. Kang, Z. Liu, W. Kuang, J. Liu and M. Zhou, *J. Appl. Polym. Sci.* 2015, **DOI: 10.1002/app.41870**

SEPARATION APPLICATIONS

Experiment and simulation of the simultaneous removal of organic and inorganic contaminants by micellar enhanced ultrafiltration with mixed micelles
A. D. Vibhandik, S. Pawar and K. V. Marathe, *J. Appl. Polym. Sci.* 2015, **DOI: 10.1002/app.41435**

Polymeric membrane modification using SPEEK and bentonite for ultrafiltration of dairy wastewater
A. Pagidi, Y. Lukka Thuyavan, G. Arthanareeswaran, A. F. Ismail, J. Jaafar and D. Paul, *J. Appl. Polym. Sci.* 2015, **DOI: 10.1002/app.41651**

Forensic analysis of degraded polypropylene hollow fibers utilized in microfiltration
X. Lu, P. Shah, S. Maruf, S. Ortiz, T. Hoffard and J. Pellegrino, *J. Appl. Polym. Sci.* 2015, **DOI: 10.1002/app.41553**

A surface-renewal model for constant flux cross-flow microfiltration
S. Jiang and S. G. Chatterjee, *J. Appl. Polym. Sci.* 2015, **DOI: 10.1002/app.41778**

Ultrafiltration of aquatic humic substances through magnetically responsive polysulfone membranes
N. A. Azmi, Q. H. Ng and S. C. Low, *J. Appl. Polym. Sci.* 2015, **DOI: 10.1002/app.41874**

BIOSEPARATIONS APPLICATIONS

Analysis of the effects of electrostatic interactions on protein transport through zwitterionic ultrafiltration membranes using protein charge ladders
M. Hadidi and A. L. Zydney, *J. Appl. Polym. Sci.* 2015, **DOI: 10.1002/app.41540**

Modification of microfiltration membranes by hydrogel impregnation for pDNA purification
P. H. Castilho, T. R. Correia, M. T. Pessoa de Amorim, I. C. Escobar, J. A. Queiroz, I. J. Correia and A. M. Morão, *J. Appl. Polym. Sci.* 2015, **DOI: 10.1002/app.41610**

Hemodialysis membrane surface chemistry as a barrier to lipopolysaccharide transfer
B. Madsen, D. W. Britt, C.-H. Ho, M. Henrie, C. Ford, E. Stroup, B. Maltby, D. Olmstead and M. Andersen, *J. Appl. Polym. Sci.* 2015, **DOI: 10.1002/app.41550**

Membrane adsorbers comprising grafted glycopolymers for targeted lectin binding
H. C. S. Chenette and S. M. Husson, *J. Appl. Polym. Sci.* 2015, **DOI: 10.1002/app.41437**

Journal of Applied Polymer Science

Fouling control through the hydrophilic surface modification of poly(vinylidene fluoride) membranes

Hanna Jang,[1] Du-Hyun Song,[1] In-Chul Kim,[1] Young-Nam Kwon[2]

[1]Research Center for Biobased Chemistry, Korea Research Institute of Chemical Technology, P. O. Box 107, Daejeon 305-600, Republic of Korea

[2]School of Urban and Environmental Engineering, Ulsan National Institute of Science and Technology, Ulsan 689-798, Republic of Korea

Correspondence to: I.-C. Kim (E-mail: ickim@krict.re.kr) and Y.-N. Kwon (E-mail: kwonyn@unist.ac.kr)

ABSTRACT: A hydrophilic fouling-resistant poly(vinyl alcohol) (PVA) based polymer was synthesized by the etherification of PVA with monochloroacetic acid under alkaline conditions, and the polymer, PVA–OCH_2COONa, was subsequently applied to modify a poly(-vinylidene fluoride) (PVDF) membrane to both enhance the hydrophilicity and provide fouling resistance. The successful etherification was confirmed by ^{13}C-NMR and attenuated total reflectance–Fourier transform infrared spectroscopy, whereas the synthesized polymer was shown by differential scanning calorimetry analysis to have an improved thermal stability over PVA. The physicochemical properties of the surfaces of the modified PVDF membranes were investigated with various analytical tools, including field emission scanning electron microscopy, atomic force microscopy, and contact angle analysis. Fouling tests with bovine serum albumin showed the PVA–OCH_2COONa modified PVDF membrane to have both a higher pure water flux and a retarded decline in flux over the filtration period compared with the PVA-coated PVDF membrane. This study demonstrated that the modification of PVDF membranes with PVA–OCH_2COONa could be an efficient method for enhancing their fouling resistance. © 2014 Wiley Periodicals, Inc. J. Appl. Polym. Sci. **2015**, *132*, 41712.

KEYWORDS: crosslinking; grafting; membranes

Received 31 August 2014; accepted 31 October 2014
DOI: 10.1002/app.41712

INTRODUCTION

Over the last few decades, membrane separation technology has made significant contributions to various fields, such as in the treatment of wastewater and drinking water and the food and medical industries.[1–3] The pressure-driven ultrafiltration (UF) process has strengths in the areas of easy operation, low power consumption, and high separation efficiency.[4–6] In the drinking water treatment industry, UF membranes with both high permeate flux and durability are required to handle large amounts of water with a small footprint. Excellent fouling resistance is also needed to prevent the performance loss of the membrane, which occurs because of the attachment of retained particles during operation over time.[4,5] Several polymers, including polyimide,[7] poly(ether imide),[8] polysulfone,[9] and poly(vinylidene fluoride) (PVDF),[10] have generally been used as membrane materials.[11,12]

Among these materials, PVDF, which has a fluorine-containing repeating unit of —$(CH_2CF_2)_n$—, has been widely used in the production of UF membranes because of its outstanding chemical resistance, good thermal stabilities, and excellent mechanical strength.[13–15] However, the applications of PVDF membranes can sometimes be limited by PVDF's vulnerability to fouling and low permeate flux because of its intrinsic hydrophobicity.[16,17] Irreversible membrane fouling, caused by the deposition and accumulation of feed components, such as suspended particles, impermeable dissolved solutes, or even solutes that are normally permeable, on the membrane surface and within the pores of the membrane reduces the operation life.[18,19] Almost all organic foulants in aqueous media tend to be hydrophobic; thus, they cluster or group together to make colloidal or suspended particles. The hydrophobic interaction that occurs between foulants and membranes causes more severe fouling problems on hydrophobic membranes than on hydrophilic ones.[20–23] Many studies have been carried out with various methods, including surface coating, surface modification by grafting hydrophilic monomers, and blending with hydrophilic polymers in a casting solution, to improve the hydrophilicity

Additional Supporting Information may be found in the online version of this article.

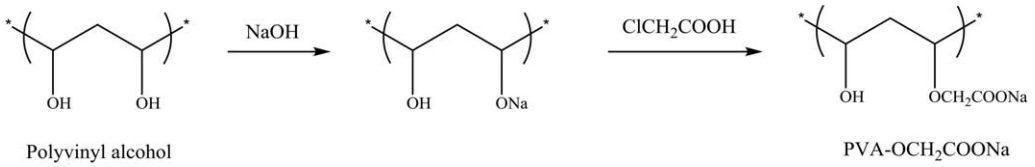

Figure 1. Schematic illustration of the process for the etherification of PVA.

and antifouling properties of the surfaces of conventional hydrophobic membranes.[24–27]

Surface coating with hydrophilic polymers is a simple but effective method for membrane surface modification, and this method has been applied extensively. Poly(vinyl alcohol) (PVA) has good fouling resistance because this polymer has a hydrophilic repeating unit of —$(CH_2CHOH)_n$—, which can be easily crosslinked by treatment with glutaraldehyde (GA).[28,29] Wang *et al.*[30] prepared a high-flux UF membrane using an electrospun PVA scaffold support in conjunction with a PVA hydrogel coating and crosslinking. The electrospun scaffold fabricated by 96% hydrolyzed PVA with a high molecular weight was demonstrated to have good mechanical performance with good tensile strength and elongation. The results indicate that the size of the hydrophilic chains connected by crosslinking points could be controlled by the degree of crosslinking in the hydrogel. The best result was reported for a GA/PVA repeat unit ratio of 0.06 to crosslink the top PVA layer. Na *et al.*[31] also developed antifouling PVA thin film composite membranes through heat treatment followed by a crosslinking reaction and drying. An increase in the concentration of PVA in the casting solution, a dynamic coating time, the GA concentration and curing time, and a decrease in the additive concentration were found to bring about a decrease in the flux and an increase in the protein rejection. The results from that study indicate that membranes modified with a PVA hydrogel layer showed remarkably high antifouling properties compared to unmodified membranes.

In this study, an anionic PVA-based polymer (PVA–OCH_2-COONa) was synthesized by the etherification of PVA with monochloroacetic acid (MCA) under alkaline conditions, and the synthesized polymer was characterized by attenuated total reflectance (ATR)–Fourier transform infrared (FTIR) spectroscopy and ^{13}C-NMR for confirmation. Subsequently, the prepared hydrophilic polymer was applied to a PVDF membrane. The high affinity of the sodium carboxymethyl group to water caused the permeate flux to increase and the ionic substances to simply be removed; this made it suitable for reducing the fouling of the membrane. The performances of the modified PVDF membranes, including the morphology, hydrophilicity, roughness, and protein fouling resistance, were systematically investigated to evaluate the feasibility of PVA–OCH_2COONa as a modification material to confer fouling resistance.

EXPERIMENTAL

Materials

PVDF (Solef 1015, molecular weight = 500,000 g/mol), purchased from Solvay (Belgium), was used as the base material for the UF membrane. Dimethyl acetamide, purchased from Samchun (Korea), was used as the solvent. Poly(vinyl pyrrolidone) (K30, molecular weight = 40,000 g/mol), purchased from Wako (Japan), was used as an additive. PVA (molecular weight = 88,000 g/mol) for the synthesis of the hydrophilic ionic polymer was purchased from Acros Organics. 2-Propanol, purchased from Samchun (Korea), was used as a reaction medium. Sodium hydroxide (NaOH) and MCA were purchased from Junsei (Japan). GA and hydrogen chloride (HCl) were purchased from Kasei Chemicals (Japan) and Aldrich, respectively, and were used for crosslinking reactions. Bovine serum albumin (BSA; molecular weight = 67,000 g/mol) was purchased from Acros Organics. The deionized water used in the experiments was produced with a Milli-Q system from Millipore.

Preparation of the Hydrophilic PVA–OCH_2COONa

PVA–OCH_2COONa was prepared and characterized with a procedure similar to that described in the literature.[32,33] Figure 1 presents the synthesis pathways through the process of alkalization and etherification. Briefly, 2 g of PVA in powder form was dissolved in 200 mL of 2-propanol under mechanical stirring. After 30 min, 30 mL of NaOH solution (0.05 mol) was added to the reaction medium. The solution was stirred continuously for 1 h, after which 0.05 mol of MCA was introduced, and the reaction was left for an additional 2 h. The resulting PVA–OCH_2COONa was filtered and dried at 60°C in a vacuum oven.

Both NMR spectroscopy and ATR–FTIR spectroscopy were used to evaluate the modification. The ^{13}C-NMR spectrum was obtained at 25°C in D_2O with a Bruker Avance 500-MHz spectrometer. The ATR–FTIR spectrum was recorded on a Nicolet 5700 FTIR spectrometer at a resolution of 4 cm^{-1} in the wavenumber range from 400 to 4000 cm^{-1}. Differential scanning calorimetry (DSC) measurement was conducted with a DSC Q1000 system under an N_2 purge with a heating rate of 10°C/min from −80 to 300°C.

Modification of the PVDF Membrane with the PVA–OCH_2COONa

PVDF flat-sheet membranes were prepared as support membranes by a phase-inversion method. A casting solution was prepared by the dissolution of 18 wt % PVDF polymer and 10 wt % poly(vinyl pyrrolidone) additive in dimethyl acetamide. The solution was mechanically stirred until the polymer was completely dissolved. The solution was then cast onto a polyester nonwoven fabric with a flat-sheet membrane casting apparatus with a gap of 250 μm. The cast film was immersed into a coagulation bath at 25°C right after casting. The membranes were kept in a circulation water bath overnight to remove residual solvent, additives, and impurities. The modification of the PVDF membranes was then conducted by the dip-coating method. The PVDF membranes were dipped into an aqueous solution containing GA (5 wt %) and HCl (0.5 wt %) in

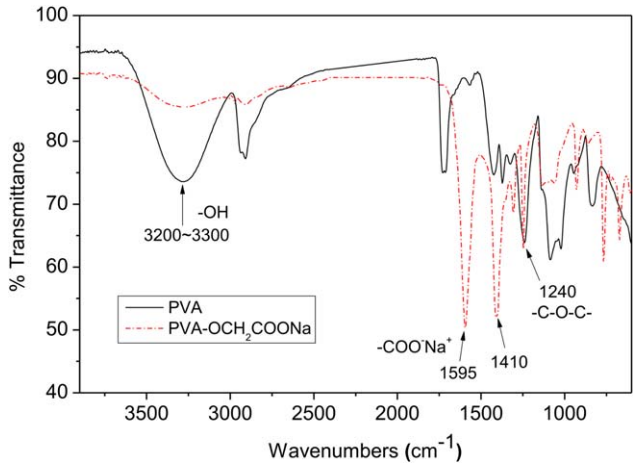

Figure 2. ATR–FTIR absorption spectra of PVA and PVA–OCH_2COONa. [Color figure can be viewed in the online issue, which is available at www.interscience.wiley.com.]

deionized water, and the excess solution was removed by squeezing with a soft rubbery roller after 1 min. The PVDF membranes were then immersed in a solution of 0.1 wt % PVA–OCH_2COONa. After 1 min of reaction, the membranes were dried in air for 1 h.

Membrane Surface Characterization

The structure and morphology of the control membrane and modified membranes were characterized by field emission scanning electron microscopy (FESEM) with a Tescan Mira 3 LMU FEG operated at an acceleration voltage of 10 kV. The FESEM samples were prepared by the vacuum sputtering of Pt onto the dried samples at room temperature. The pore sizes of the membranes were determined with a capillary flow porometer (Porous Materials, Inc., CFP-1200-AE). The membranes were first dipped in a wetting agent, Galwick. Nitrogen gas flow was used to displace the liquid from the pores, and the pressure required to empty the most constricted part of the pores was measured. The mean flow pore size corresponded to the pore size calculated at the pressure where the wet curve and the half dry curve met. The water contact angles used to measure the hydrophilic properties of the surface-modified membranes were measured and calculated in static mode on an SEO Phoenix 300A at room temperature. One drop of water (3 μL) was delivered on the surface of the film with an automatic piston syringe and then photographed. The reported contact angles were averaged from at least triplicate three-time determinations carried out at random locations. The surface morphologies of the control and modified membranes were imaged by atomic force microscopy (AFM) with a Bruker Dimension Icon Nanoscope V. We acquired the AFM images of 5-μm scans by scanning the sample in air under ambient laboratory conditions. The surface roughness was then assessed.

Pure Water Flux (J_0) and BSA Fouling Experiments

UF experiments were carried out for the prepared membranes in a batch-type, dead-end cell with a model 8200 instrument from Amicon. The effective membrane area available for UF was 28.26 cm^2, with a diameter of 62 mm. After the membranes were prepressured under 3 kgf/cm^2 for 120 min, J_0 was also measured under fixed conditions until the steady-state flux was obtained by the collection of the volume of the permeated water under 1 kgf/cm^2 per every 1 min. When the steady-state flux was reached, a 20-ppm BSA solution was forced to permeate through the membrane according to the same procedure discussed previously, and the flux was recorded as J.

RESULTS AND DISCUSSION

Characterization of the Hydrophilic PVA–OCH_2COONa

A hydrophilic fouling-resistant PVA-based polymer was prepared by the etherification of PVA with MCA under alkaline conditions. Figure 2 shows the ATR–FTIR spectra of PVA–OCH_2COONa in comparison with PVA. PVA showed the characteristic peaks of O—H, CH_2, CH, and C—C bonds. A strong and broad O—H stretching peak was observed in the region 3200 to 3300 cm^{-1}. Antisymmetric and symmetric stretching bands of CH_2 occurred at 2942 and 2905 cm^{-1}, respectively, and a CH stretching vibration peak appeared at 2834 cm^{-1}. The residual carbonyl bands at 1714 and 1566 cm^{-1} of PVA showed that the PVA was formed by the hydrolysis of poly(vinyl acetate) during the manufacturing process. The symmetric bending mode of CH_2 was found at 1424 cm^{-1}. The bands at about 1323 and 1240 cm^{-1} were attributed to the wagging

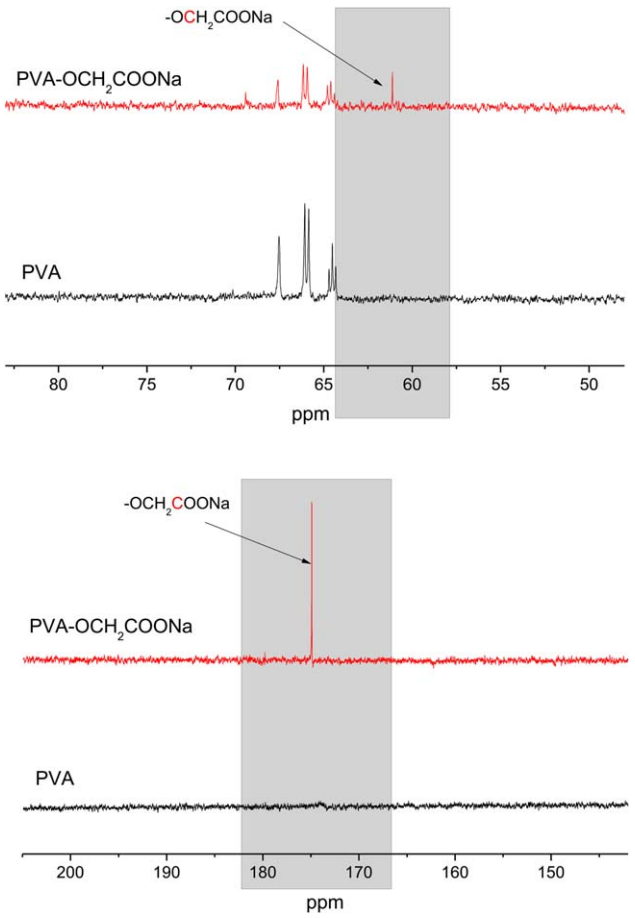

Figure 3. ^{13}C-NMR spectra of PVA and PVA–OCH_2COONa. [Color figure can be viewed in the online issue, which is available at www.interscience.wiley.com.]

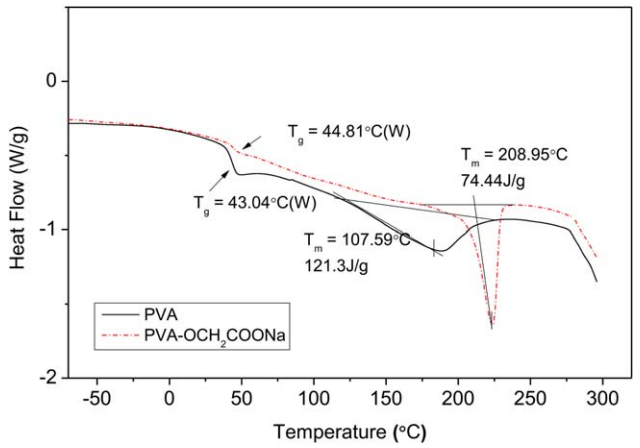

Figure 4. DSC thermograms of PVA and PVA–OCH_2COONa. [Color figure can be viewed in the online issue, which is available at www.interscience.wiley.com.]

vibrations of CH_2 and CH, respectively. The band at about 1084 cm^{-1} was due to the C—O stretching vibration of the ether group, whereas the band at 945 cm^{-1} was related to the syndiotactic structure of PVA. The bands at 833 and 652 cm^{-1} were assigned to the C—C stretching vibrations and out-of-plane OH bending, respectively.[34] PVA–OCH_2COONa, however, showed distinct differences in the ATR–FTIR spectra. The band ranging from 2800 to 3300 cm^{-1} was similar to that found in PVA, but its intensity decreased remarkably because of the etherification. Significant absorption bands were observed at 1595 and 1410 cm^{-1}; this was attributed to the lone-pair electrons of carboxylate and consequent resonance delocalization of the π bond, which indicated the presence of symmetric and asymmetric carboxylate anions (COO^-).[35] The bands around 1240 cm^{-1} were assigned to the C—O—C ether group but may have also overlapped with the CH vibration absorption. ^{13}C-NMR analysis provided additional evidence for the successful modification of PVA–OCH_2COONa. The ^{13}C-NMR spectra of PVA and the synthesized PVA–OCH_2COONa are shown in Figure 3. In comparison with the spectrum of PVA in D_2O solution, PVA–OCH_2COONa was observed to have new peaks at δ about 60 and 175 ppm; these were assigned to the carbon atoms attributed to the C—O and C═O groups, respectively. These effects are cumulative, so the presence of more electronegative groups resulted in more deshielding and, therefore, larger chemical shifts. Electronegative groups decreased the electron density around the carbons and provided less shielding (i.e., deshielding); this caused the chemical shift to increase. The carbon atom in a carbonyl group has a relatively low electron density around it and, thus, is relatively deshielded. Consequently, it has a higher chemical shift than most other types of carbons. The DSC endothermic profiles showed the glass-transition temperature (T_g) of PVA at 43.04°C, whereas that of PVA–OCH_2COONa occurred at 44.81°C (Figure 4). DSC analysis indicated that PVA–OCH_2COONa, with a melting temperature (T_m) of 208.95°C, was more thermally stable than PVA, which melted at 107.59°C.

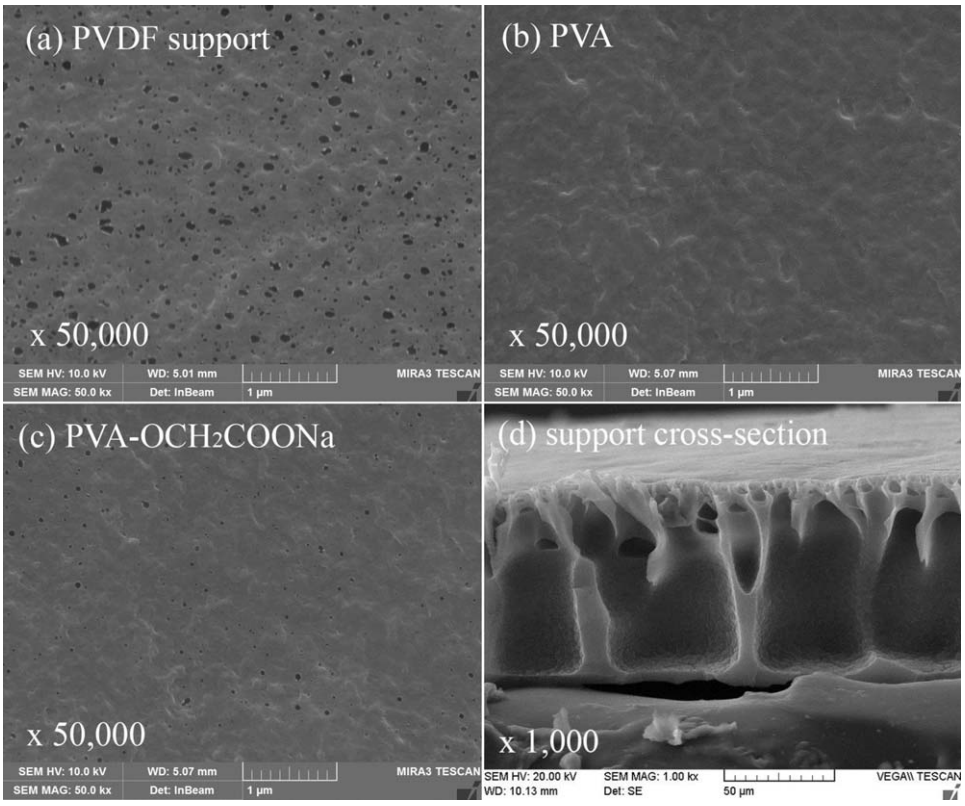

Figure 5. FESEM images of the membrane surfaces: (a) PVDF support membrane, (b) PVDF coated with PVA, (c) PVDF coated with PVA–OCH_2COONa, and (d) cross section of the PVDF support membrane.

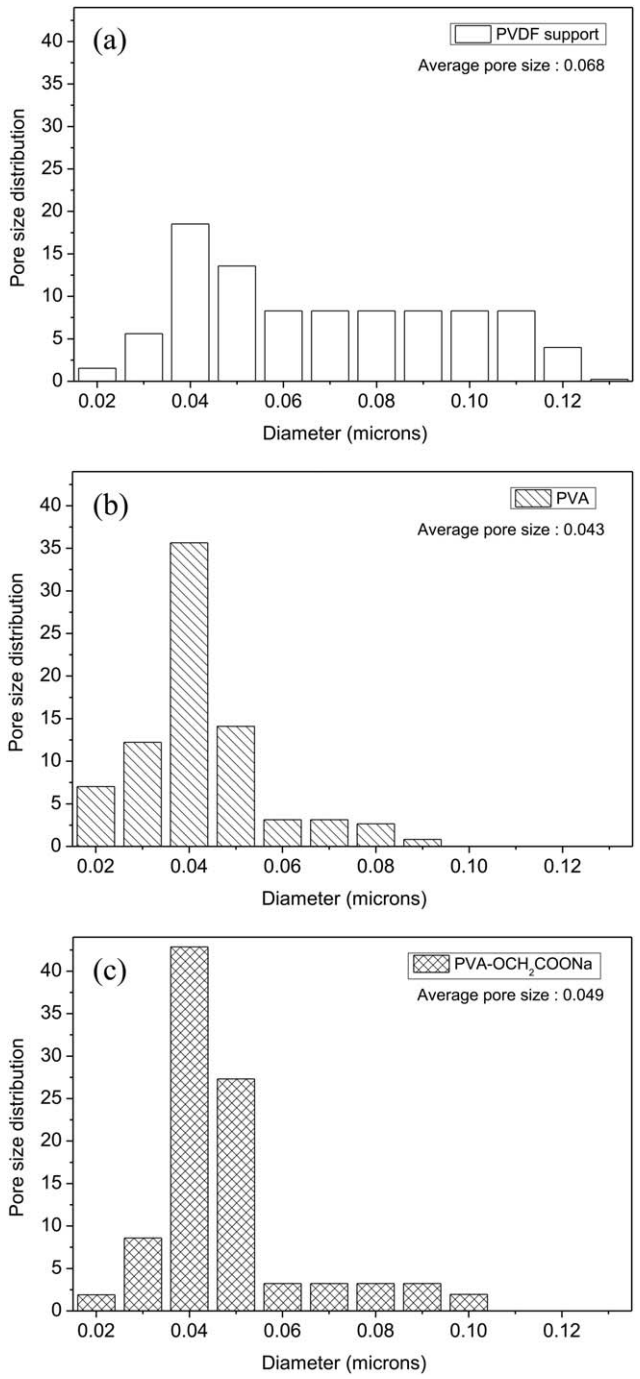

Figure 6. Pore size distributions: (a) PVDF support membrane, (b) PVDF coated with PVA, and (c) PVDF coated with PVA–OCH_2COONa.

Characterization of the Modified PVDF Membranes

FESEM images of the surfaces of the PVDF membrane and the membranes modified with PVA and PVA–OCH_2COONa under 50,000× magnification are shown in Figure 5. The average pore size was found to decrease significantly after modification of the hydrophobic PVDF membrane. The PVDF control membrane had an average pore size of 0.068 μm, whereas the PVA-modified membrane and PVA–OCH_2COONa-modified membrane had average pore sizes of 0.043 and 0.049 μm, respectively. Figure 6 shows the pore size distribution of the membranes.

AFM surface analysis of the membranes was conducted with dry samples. The average roughness (R_a) indicates the arithmetic average of the absolute values of the surface height deviations from the center plane. As shown in Figure 7, the surface of the PVDF membrane was originally quite rough and was composed of mountainous peaks. The R_a of the PVDF membrane was 26.7 ± 0.5 nm. In contrast, the R_a values of the PVA-modified and PVA–OCH_2COONa-modified membranes were 16.4 ± 0.2 and 14.1 ± 0.2 nm, respectively. These results demonstrate that the modified PVDF membranes became smoother and had a lower roughness; this implied a thin layer of the PVA, and PVA–OCH_2COONa was formed on top of the membrane. These results were consistent with the scanning electron

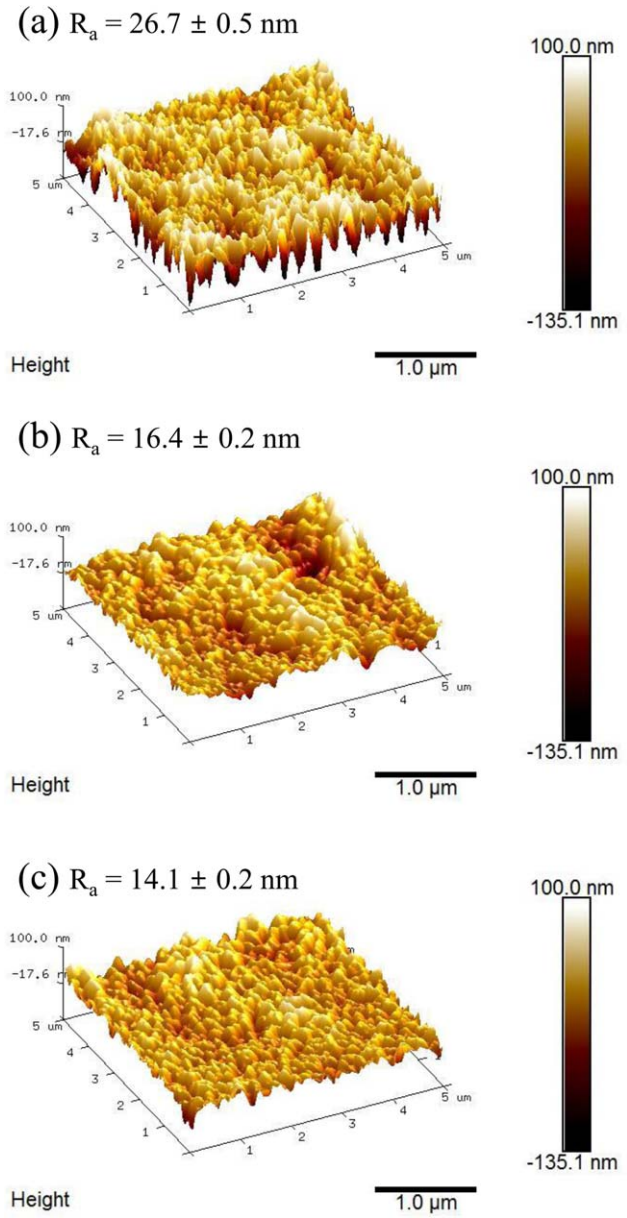

Figure 7. AFM images of the membrane surfaces: (a) PVDF support membrane, (b) PVDF coated with PVA, and (c) PVDF coated with PVA–OCH_2COONa [R_a (nm)]. [Color figure can be viewed in the online issue, which is available at www.interscience.wiley.com.]

Table I. Contact Angles of the PVDF Support Membrane, PVDF Coated with PVA, and PVDF Coated with PVA–OCH_2COONa

Membrane	Support (PVDF)	PVA	PVA–OCH_2COONa
Contact angle (°)	60.51	47.50	44.34

microscopy (SEM) observations, and the smoothed surface morphology was expected to improve the antifouling capabilities of the PVDF membrane. However, the coating layer applied in this study was thin enough not to show a discernible peak pattern in ATR–FTIR spectroscopy compared with the bare membrane (Supporting Information, Figure S1).

The surface hydrophilicity is one of the most important factors in determining the antifouling properties of UF membranes. Hydrophobic membranes have nonpolar groups and lower surface free energy; this can prevent contact with water and can push out the water molecules adjoining it.[36] The hydrophilicity of the membranes synthesized in this study was evaluated by contact angle measurement, which has commonly been used to assess the wettability and interfacial energy of the substrate surfaces. Table I shows the contact angle values of the PVDF membrane and the membranes modified with PVA and PVA–OCH_2COONa. The contact angle was observed to decrease significantly after the modification of the hydrophobic PVDF. The original PVDF membrane had an average contact angle of 60.51°; this decreased to 44.34° when the membrane was coated with 0.1 wt % PVA–OCH_2COONa. This phenomenon was attributed to the hydrophilic nature of the hydroxyl groups and the sodium carboxymethyl groups. The decrease in the contact angle indicated the creation of a highly hydrophilic surface. The contact angle of the membrane coated with PVA was slightly higher than that of the membrane coated with PVA–OCH_2COONa. This was likely due to the different water affinities of the hydroxyl and sodium carboxymethyl groups.

DSC analysis was conducted to indicate that the difference between the PVA and synthesized PVA–OCH2COONa. The enhanced thermal stability shown in Figure 4 was not directly related to the membrane performance.

Fouling of Membranes by BSA

The antifouling propensity of the virgin and modified membranes was evaluated by the filtration of a 20-ppm BSA solution through the membranes. J_0 of the PVDF membrane was 1965 L/m^2 h. However, the modification of the membrane with the hydrophilic PVA and PVA–OCH_2COONa led to declines in J_0 of the membranes by up to 155 and 200 L/m^2 h. The decline of J_0 after surface modification was likely due to the pore size change and additional coating layer; these caused additional resistance for water molecules passing through the membrane, as shown in Figures 5 and 6.[36] Figure 8 shows the normalized flux of the unmodified membrane and the membranes modified with PVA and PVA–OCH_2COONa. The normalized flux is the ratio of the momentary BSA flux (J) divided by J_0. The decline of the flux in the unmodified membrane was clearly much higher than those in the modified membranes. The fast decline in the flux of the unmodified membrane was likely affected by its larger pore size and its surface hydrophobicity. The fouling of membranes with large pore sizes occurred easily because of the higher concentration polarization and easy pore blocking, and the hydrophobic nature of the PVDF membrane induced a higher fouling tendency. In the case of the membrane modified with PVA–OCH_2COONa, fouling with BSA was shown to decrease remarkably; this provided high permeate flux because of the high hydrophilic affinity and reduced roughness. After continuous operation for 120 min, the normalized flux (J/J_0) declined to 2% for the PVDF membrane, whereas it was still sustained at 48% for the membrane modified with PVA–OCH_2COONa. The PVA–OCH_2COONa-coated membrane showed both a high permeate flux and excellent antifouling compared to the PVA-coated membrane because of the enhanced hydrophilic and anionic nature of the attached functional group. The surface of the membrane with the introduced hydrophilic sodium methyl carboxyl groups was negatively charged, whereas BSA, with an isoelectric point of pH 4.8, also had a negative charge at neutral pH.[30] The interaction between two likely charged materials is repulsive. The BSA near the negatively charged membrane surface was easily excluded by electrostatic repulsion. Both the charge repulsion and enhanced

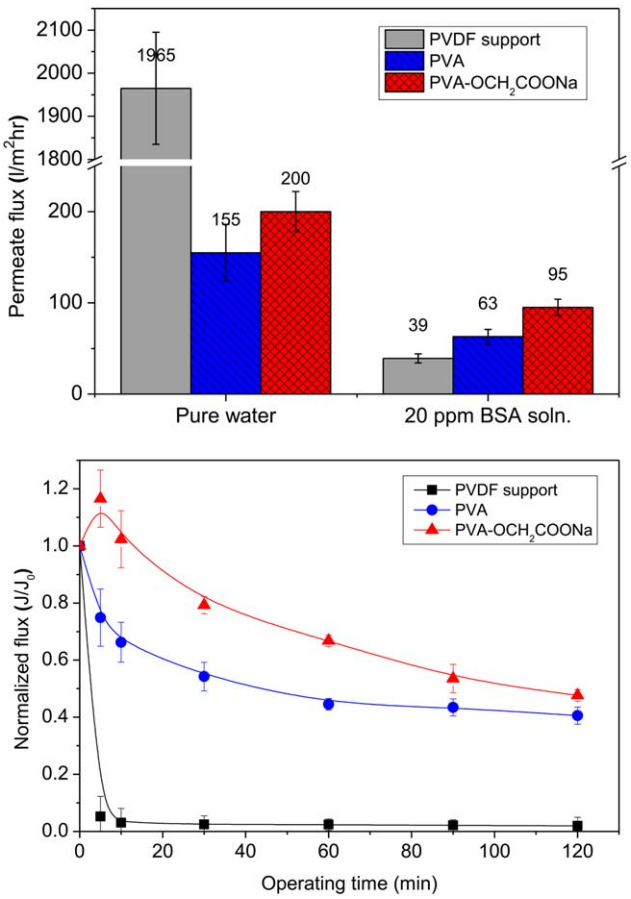

Figure 8. Permeate fluxes and normalized fluxes of the membranes coated with PVA and PVA–OCH_2COONa versus the unmodified membrane. The flux was measured at 1 kgf/cm^2 with a 20-ppm BSA aqueous solution. [Color figure can be viewed in the online issue, which is available at www.interscience.wiley.com.]

hydrophilicity of the PVA–OCH_2COONa coated membrane reduced the degree of protein adsorption to the membrane surface. Therefore, the PVDF membrane could be most efficiently modified through the coating of the surface with PVA–OCH_2-COONa to enhance its surface hydrophilicity and fouling resistance. The rejection of 20-ppm BSA by the PVDF was negligible, but PVA-coated and PVA–OCH_2COONa membranes showed rejections of about 21 and 39%, respectively.

CONCLUSIONS

A hydrophilic PVA–OCH_2COONa polymer was successfully synthesized through the etherification of PVA with chloroacetic acid in alkaline medium, as confirmed by the ATR–FTIR and ^{13}C-NMR spectra. Hydrophilically modified PVDF membranes were prepared by the surface coating method with a crosslinking agent. SEM and PMI confirmed that the modified PVDF membranes had a reduced pore size, whereas contact angle measurement indicated that the modified PVDF membranes had very good hydrophilicity. The modified PVDF membrane was also found to be smoother with lower roughness, as observed by AFM. The introduction of sodium carboxymethyl groups into PVA led to an increase in excellent antifouling properties because of the high hydrophilicity and electronegativity of the sodium carboxymethyl groups. We believe that the superior performance of PVDF membranes coated with PVA–OCH_2COONa will have great potential for practical applications.

ACKNOWLEDGMENTS

This research was supported by the World Premier Materials Program through the Ministry of Trade, Industry, and Energy.

REFERENCES

1. Mohammadi, T.; Esmaeelifar, A. *J. Membr. Sci.* **2005**, *254*, 129.
2. Rahimpour, A.; Madaeni, S. S.; Amirinejad, M.; Mansourplanah, Y.; Zereshki, S. *J. Membr. Sci.* **2009**, *330*, 189.
3. Huang, J.-H.; Zeng, G.-M.; Fang, Y.-Y.; Qu, Y.-H.; Li, X. *J. Membr. Sci.* **2009**, *326*, 303.
4. Katsou, E.; Malamis, S.; Haralambous, K. J.; Loizidou, M. *J. Membr. Sci.* **2010**, *360*, 234.
5. Cassano, A.; Molinari, R.; Romano, M.; Drioli, E. *J. Membr. Sci.* **2001**, *181*, 111.
6. Cano, G.; Steinle, P.; Daurelle, J. V.; Wyart, Y.; Glucina, K.; Bourdiol, D.; Moulin, P. *J. Membr. Sci.* **2013**, *431*, 221.
7. Kim, I. C.; Kim, J. H.; Lee, K. H.; Tak, T. M. *J. Membr. Sci.* **2002**, *205*, 113.
8. Bowen, W. R.; Cheng, S. Y.; Doneva, T. A.; Oatley, D. L. *J. Membr. Sci.* **2005**, *250*, 1.
9. Sinha, M. K.; Purkait, M. K. *J. Membr. Sci.* **2014**, *464*, 20.
10. Zhang, Y.; Zhao, J.; Chu, H.; Zhou, X.; Wei, Y. *Desalination* **2014**, *344*, 71.
11. Zeman, L. J.; Zydney, A. L. Microfiltration and Ultrafiltration: Principles and Applications; CRC: Boca Raton, FL, **1996**.
12. Liu, F.; Xu, Y.-Y.; Zhu, B.-K.; Zhang, F.; Zhu, L.-P. *J. Membr. Sci.* **2009**, *345*, 331.
13. Kang, G.-D.; Cao, Y.-M. *J. Membr. Sci.* **2014**, *463*, 145.
14. Liu, F.; Hashim, N. A.; Liu, Y.; Abed, M. R. M.; Li, K. *J. Membr. Sci.* **2011**, *375*, 1.
15. Porter, M. C. Handbook of Industrial Membrane Technology; Noyes: Saddle River, NJ, **1991**.
16. Mulder, M. Basic Principles of Membrane Technology; Springer: New York, **1996**.
17. Peter-Varbanets, M.; Margot, J.; Traber, J.; Pronk, W. *J. Membr. Sci.* **2011**, *377*, 42.
18. Drioli, E.; Giorno, L. Comprehensive Membrane Science and Engineering; Elsevier Science: Amsterdam, **2010**.
19. Cho, Y. H.; Kim, H. W.; Nam, S. Y.; Park, H. B. *J. Membr. Sci.* **2011**, *379*, 296.
20. Sui, Y.; Wang, Z.; Gao, X.; Gao, C. *J. Membr. Sci.* **2012**, *413*, 38.
21. Cheryan, M. Ultrafiltration and Microfiltration Handbook; CRC: Boca Raton, FL, **1998**.
22. Chen, X.; He, Y.; Shi, C.; Fu, W.; Bi, S.; Wang, Z.; Chen, L. *J. Membr. Sci.* **2014**, *469*, 447.
23. He, Y.; Chen, X.; Bi, S.; Fu, W.; Shi, C.; Chen, L. *React. Funct. Polym.* **2014**, *74*, 58.
24. Koh, J. K.; Kim, Y. W.; Ahn, S. H.; Min, B. R.; Kim, J. H. *J. Polym. Sci. Part B: Polym. Phys.* **2010**, *48*, 183.
25. Liang, S.; Qi, G.; Xiao, K.; Sun, J.; Giannelis, E. P.; Huang, X.; Elimelech, M. *J. Membr. Sci.* **2014**, *463*, 94.
26. Xu, Z.; Zhang, J.; Shan, M.; Li, Y.; Li, B.; Niu, J.; Zhou, B.; Qian, X. *J. Membr. Sci.* **2014**, *458*, 1.
27. Zhang, Y. Z.; Li, H. Q.; Li, H.; Li, R.; Xiao, C. F. *Desalination* **2006**, *192*, 214.
28. Bolto, B.; Tran, T.; Hoang, M.; Xie, Z. *Prog. Polym. Sci.* **2009**, *34*, 969.
29. Ma, X.; Su, Y.; Sun, Q.; Wang, Y.; Jiang, Z. *J. Membr. Sci.* **2007**, *300*, 71.
30. Wang, X.; Fang, D.; Yoon, K.; Hsiao, B.; Chu, B. *J. Membr. Sci.* **2006**, *278*, 261.
31. Na, L.; Liu, Z. Z.; Xu, S. G. *J. Membr. Sci.* **2000**, *169*, 17.
32. Wakelyn, P. J.; Bertoniere, N. R.; French, A. D.; Thibodeaux, D. P.; Triplett, B. A.; Rousselle, M.-A.; Goynes, W. R., Jr.; Edwards, J. V.; Hunter, L.; McAlister, D. D.; Gamble, G. R. Cotton Fiber Chemistry and Technology; CRC: Boca Raton, FL, **2006**.
33. Yu, C.; Li, B. *Polym. Compos.* **2008**, *29*, 998.
34. Shehap, A. M. *J. Solids* **2008**, *31*, 75.
35. Nyquist, R. A. Interpreting Infrared, Raman, and Nuclear Magnetic Resonance Spectra; Academic: Waltham, MA, **2001**.
36. Zhang, H.; Li, H.; Yang, F.; Wang, T.; Gao, J.; Jiang, T. *Sep. Purif. Technol.* **2011**, *77*, 162.